

ATB 63914

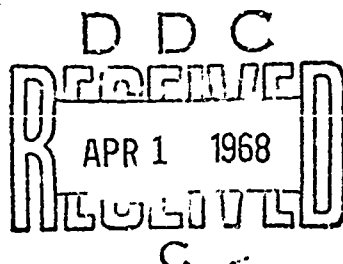
A Study of Buckling and Snapping Under Dynamic Load

DECEMBER 1967

Prepared by M. H. LOCK
Applied Mechanics Division

Laboratory Operations
AEROSPACE CORPORATION

Prepared for SPACE AND MISSILE SYSTEMS ORGANIZATION
AIR FORCE SYSTEMS COMMAND
LOS ANGELES AIR FORCE STATION
Los Angeles, California



THIS DOCUMENT HAS BEEN APPROVED FOR PUBLIC
RELEASE AND SALE; ITS DISTRIBUTION IS UNLIMITED

Air Force Report No.
SAMSO TR-68-100

Aerospace Report No.
TR-0158(3240-30)-3

A STUDY OF BUCKLING AND SNAPPING
UNDER DYNAMIC LOAD

Prepared by
M. H. Lock
Applied Mechanics Division

Laboratory Operations
AEROSPACE CORPORATION
El Segundo, California

December 1967

Prepared for
SPACE AND MISSILE SYSTEMS ORGANIZATION
AIR FORCE SYSTEMS COMMAND
LOS ANGELES AIR FORCE STATION
Los Angeles, California

This document has been approved for public
release and sale; its distribution is unlimited

FOREWORD

This report is published by the Aerospace Corporation, El Segundo, California, under Air Force Contract No. F04695-67-C-0158. The report was authored by M. H. Lock of the Applied Mechanics Division, Aerospace Corporation.

This report documents research carried out from August 1966 to August 1967 and was submitted on 7 February 1968 to Lt. Dennis R. Cochran, SMTTM, for review and approval.

The author expresses thanks to Mr. Gerald Keerbs of the Computation and Data Processing Center for assistance in the numerical phases of this study.

Approved



W. F. Radcliffe, Director
Engineering Sciences Subdivision
Applied Mechanics Division



R. A. Hartunian, Director
Aerodynamics Propulsion and
Research Laboratory
Laboratory Division

Publication of this report does not constitute Air Force approval of the report's findings or conclusions. It is published only for the exchange and stimulation of ideas.



Dennis R. Cochran, Lt., USAF
Project Officer

ABSTRACT

The behavior of a shallow arch and a thin ring under a dynamic pulse loading is studied for a wide range of geometric and load parameters. The nonlinear dynamic response and static load deflection characteristics of the systems are related and employed to define dynamic elastic snapping and dynamic elastic buckling. When such a relationship cannot be established, the mechanism of dynamic elastic-plastic buckling is introduced. Critical dynamic load criteria are specified, and critical dynamic load data are developed as a function of structural geometry and load duration. Finally, a classification scheme for dynamic load problems is suggested.

NOMENCLATURE

A = area of the arch cross-section
 $a_n(\tau)$ = generalized coordinate describing nondimensional transverse displacement of the arch
 $c_m(\tau)$ = generalized coordinate describing circumferential displacement of the ring in m^{th} nonsymmetric mode
E = Young's modulus
e = ratio of initial height of arch to radius of gyration of arch cross-section
 g = (pR/Eh) , nondimensional pressure parameter in the ring problem
 \bar{g} = critical value of g required for static buckling
 g^* = critical value of g required for dynamic buckling
h = thickness of the ring or arch
 I = $\int_0^{\tau_d} q d\tau$, impulse parameter in arch problem
 J = $\int_0^{\tau_d} g d\tau$, impulse parameter in ring problem
k = radius of gyration of the arch cross-section
L = span of the arch
p = pressure load
 q = $(p/EAk^3)(L/\tau)^4$, nondimensional pressure load in arch problem
 q_1 = amplitude of nondimensional pressure load acting upon the arch (see Eq. 1)
 \bar{q}_1 = critical value of q_1 required to produce snapping under a static pressure load
 q_1^* = critical value of q_1 required for snapping under a dynamic pressure load
R = radius of the ring
 $r_o(\)$ = generalized coordinate describing nondimensional radial displacement in axisymmetric mode

$r_m(\tau)$ = generalized coordinate describing nondimensional radial displacement of the ring in m^{th} nonsymmetric mode
 t = time
 $v(\theta, \tau)$ = circumferential displacement of the ring (see Figure 1b)
 $w(\xi, \tau)$ = transverse position of the middle surface of the arch (see Figure 1a)
 $w(\theta, \tau)$ = radial displacement of the ring (see Figure 1b)
 x = Cartesian coordinate along span of the arch (see Figure 1a)
 $\zeta(\theta, \tau)$ = $w(\theta, \tau)/R$, nondimensional radial displacement of the ring
 $\eta(\xi, \tau)$ = $w(\xi, \tau)/k$, nondimensional transverse position of the middle surface of the arch
 θ = angular coordinate for the ring (see Figure 1b)
 ξ = x/L nondimensional Cartesian coordinate for the arch
 ρ_s = mass density
 σ_y = yield stress
 τ = $(1/R)(E/\rho_s)^{1/2} t$, nondimensional time in the ring problem
 τ = $(\pi/L)^2(EAk^2/\rho_s h)^{1/2} t$, nondimensional time in the arch problem
 τ_0 = dimensionless period of the axisymmetric mode of the ring
 τ_1 = dimensionless period of the fundamental symmetric mode of the arch
 τ_d = nondimensional duration of the pressure load
 $\psi(\theta, \tau)$ = $v(\theta, \tau)/R$, nondimensional circumferential displacement of the ring

CONTENTS

FOREWORD	ii
ABSTRACT.....	iii
NOMENCLATURE	iv
1. INTRODUCTION	1
2. STATIC LOAD PROBLEM.....	6
3. DYNAMIC LOAD PROBLEM.....	12
4. COMPARISON OF CRITICAL LOADS.....	30
5. COMPARISON WITH RELATED WORK	31
6. CONCLUDING REMARKS.....	34
APPENDIX: PARTIAL DIFFERENTIAL EQUATIONS OF MOTION ..	A-1
REFERENCES.....	R-1

FIGURES

1a.	Shallow Sinusoidal Arch Problem	2
1b.	Circular Ring Problem	3
2.	Time History of Dynamic Pressure Load	5
3.	Static Load Deflection Curves for Shallow Arch	8
4.	Static Load Deflection Curves for Circular Ring	10
5.	Variation of $ a_1 _{\max}$ with Load Parameter: $e = 10$	14
6.	Variation of Critical Step Load with Arch Geometry	16
7.	Response of Arch to Supercritical Step Load: $e = 4$	17
8.	Response of Arch to Supercritical Step Load: $e = 10$	18
9.	Variation of Critical Load Ratio with Load Duration	20
10.	Variation of Critical Impulse Parameter with Arch Geometry	21
11.	Variation of $ r_m _{\max}$ with Load Parameter: $R/h = 129$, $m = 5$	23
12.	Response of Circular Ring to Step Load: $R/h = 12.9$, $m = 5$	25
13.	Variation of $ r_m _{\max}$ with Impulse Level: $R/h = 129$, $m = 15$	26
14.	Variation of Critical Impulse Parameter with Ring Geometry	28
15.	Typical Variation of Critical Load Ratio with Load Duration: $R/h = 129$	29
16.	Classification System	35

DISCLAIMER NOTICE

**THIS DOCUMENT IS BEST QUALITY
PRACTICABLE. THE COPY FURNISHED
TO DTIC CONTAINED A SIGNIFICANT
NUMBER OF PAGES WHICH DO NOT
REPRODUCE LEGIBLY.**

OR ARE
Blank pg.
that have
been removed

**BEST
AVAILABLE COPY**

1. INTRODUCTION

Certain types of elastic structure can exhibit instability when they are subjected to static loads of sufficient magnitude. Since this phenomenon can coincide with excessive deformation or with severe degradation of structural stiffness, it is of considerable practical importance in structural design. As a result, a substantial amount of literature on the subject has been published (see References 1-4 for extensive bibliographies). Primarily these publications deal with determination of the critical levels of static load at which instability is exhibited. Such loads may be referred to as critical instability loads. If they also correspond to a significant degradation in the capability of the structure, they may be termed critical structural loads.

This report is concerned with a related problem: namely, the behavior of such structures when the external loading is time-dependent. In particular, we wish to determine critical levels of dynamic load for "typical" structural systems and to see how these dynamic loads compare with the corresponding critical static loads.

The selection of the typical structural systems is based upon elastic stability theory. Since a major part of this theory deals with perfect elastic structures* that either "snap" or "buckle" under static load (these phenomena are reviewed in the following section), it was decided to select a simple example of each of these categories. The selected systems are the shallow arch (see Figure 1a) and the thin circular ring (see Figure 1b), both structures being subject to an external compressive pressure load.

The first problem represents a "snapping" system, while the second represents a "buckling" system. The arch is assumed to be simply supported, to

* We consider a structure to be perfect if the critical static load can be obtained as an eigenvalue of the conventional equilibrium path bifurcation analysis.

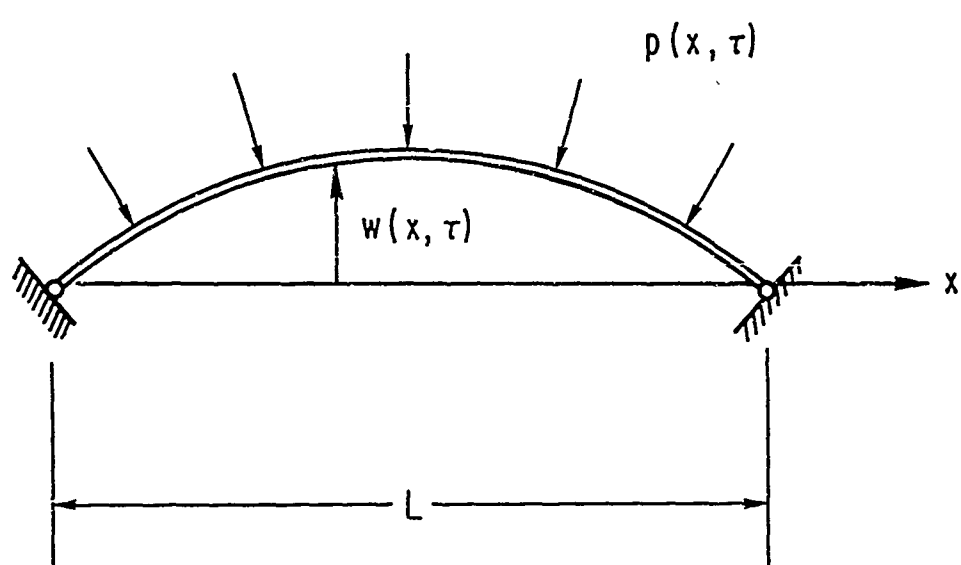


Figure 1a. Shallow Sinusoidal Arch Problem

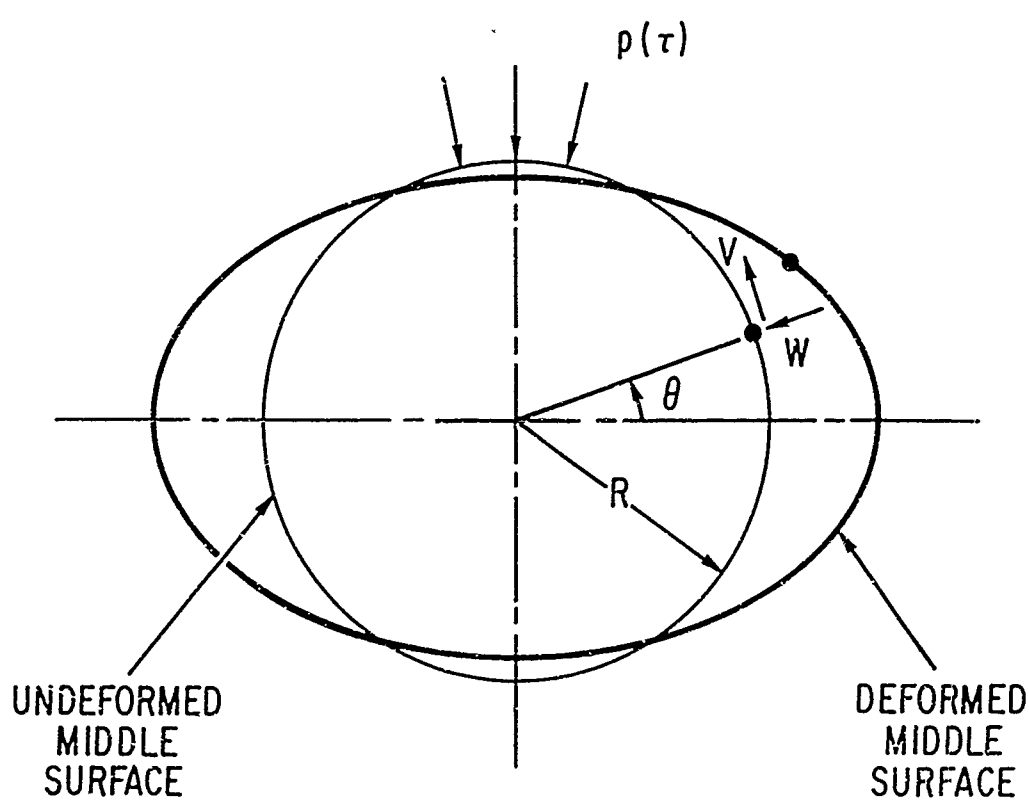


Figure 1b. Circular Ring Problem

have an initial sinusoidal shape, and to be of uniform thickness; the circular ring is also assumed to be of uniform thickness and of rectangular cross-section. The material of the two structures is assumed to be linearly elastic.

The time history of the external pressure loading was selected to be as shown in Figure 2, i.e., the load is applied instantaneously and maintained at a constant level for a specified interval of time τ_d . The duration of this loading is allowed to vary between the limits of zero (impulsive load) and infinity (step load). The spatial distribution of the load is assumed to be sinusoidal in the case of the arch and uniform in the case of the ring.

The critical values of the dynamic load are defined upon the basis of the nonlinear structural response. These loads are determined over the specified range of pulse loads for a wide range of the arch and ring geometric parameters. Finally, the critical dynamic loads are compared with the corresponding critical static loads.

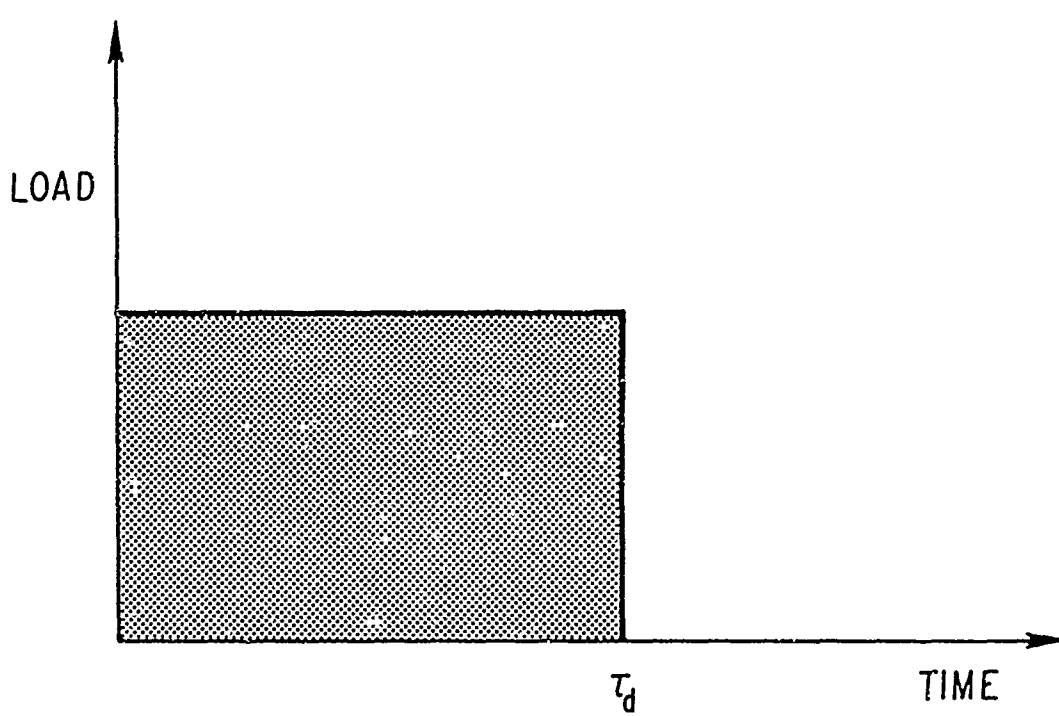


Figure 2. Time History of Dynamic Pressure Load

2. STATIC LOAD PROBLEM

Before embarking upon the determination of the dynamic response of the two systems, we will first briefly review the analysis and results of the corresponding static load problem. This review will enable us to illustrate the behavior of snapping and buckling structures and will provide the critical static loads required for comparison with the corresponding critical dynamic load results. This analytical approach consists of determining the equilibrium states of the two systems and then examining the stability of these states with respect to infinitesimal perturbations. The stability analysis yields a critical instability load, which is defined as the lowest load at which the initial equilibrium path (i.e., the path that emanates from the unloaded state) becomes unstable. Examination of the post-critical behavior of the systems then indicates whether the critical instability loads can be considered as critical loads for the structure.

2.1 SHALLOW ARCH

In the example of the shallow arch, the external pressure load is

$$q = q_1 \sin \xi \quad (1)$$

Following References 5 and 6, the transverse position $\eta(\xi)$ of the middle surface of the arch is represented by

$$\eta(\xi) = e \sin \xi + a_1 \sin \xi + a_2 \sin 2\xi \quad (2)$$

where the term $e \sin \xi$ describes the initial shape of the arch (see Nomenclature for definitions). The generalized coordinates a_1 and a_2 denote the amplitude of the displacement in the fundamental symmetric and nonsymmetric modes, respectively. The nonlinear algebraic equations governing the equilibrium states of the system were solved in References 5 and 7. It was found that the equilibrium states involve only the symmetric mode $a_1 \sin \xi$ for $0 \leq e \leq \sqrt{22}$, i.e., the generalized coordinate a_2 is identically equal to zero

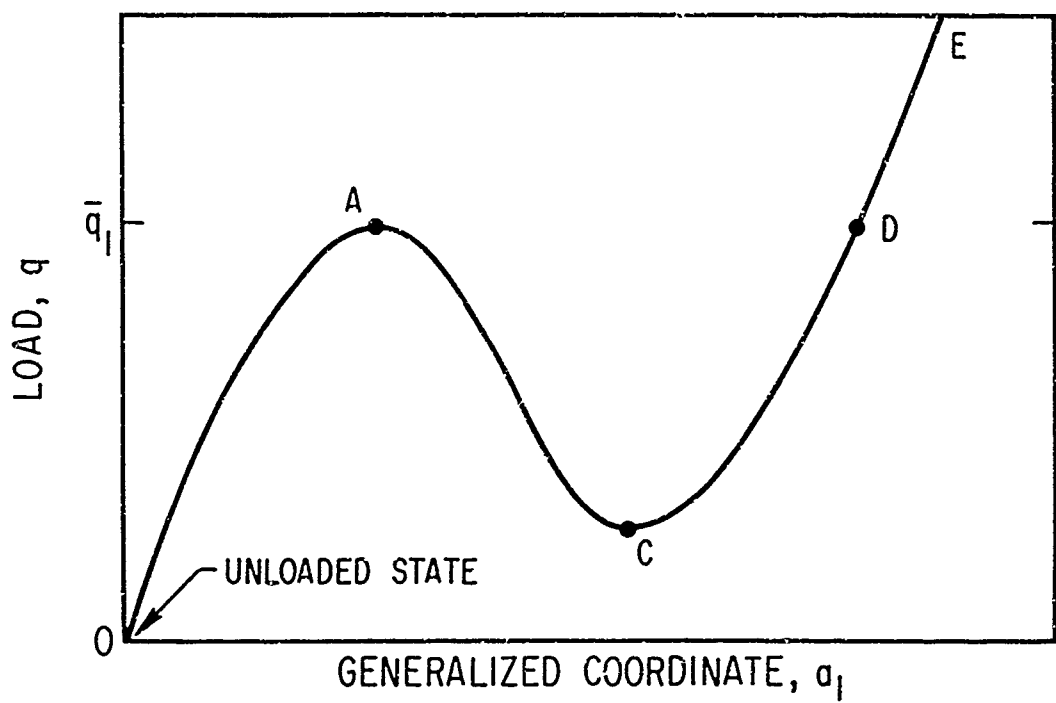
in this range; whereas, for $e > \sqrt{22}$, distinct symmetric and nonsymmetric equilibrium states co-exist for certain ranges of the load parameter q . Typical static load deflection curves for the ranges $2 < e \leq \sqrt{22}$ and $e > \sqrt{22}$ are illustrated in Figures 3a and 3b, respectively. The solid curves in these figures describe the symmetric mode equilibrium states, while the dashed line in Figure 3b represents the symmetric mode component of the nonsymmetric equilibrium states (i.e., states with $a_1 \neq 0, a_2 \neq 0$).

We consider compressive pressure loads $q \geq 0$, and for convenience we limit our considerations to the range $0 \leq e \leq 20$. For $0 \leq e \leq 2$, it is found that the static deflection is a single-valued function of the load and that the associated equilibrium states are always stable. For $2 < e \leq \sqrt{22}$, the arch becomes unstable with respect to symmetric mode perturbations at the extremum of the load deflection curve (point A in Figure 3a). Under such conditions the arch snaps through and vibrates about a large deflection equilibrium state (point D in Figure 3a); these large deflection states are stable and are referred to as snapped equilibrium states (the branch CDE of each curve shown in Figure 3 is the snapped branch of the load deflection curve). The phenomenon in this case involves only the symmetric mode and is referred to as "snapping." The critical value of the load parameter at which instability occurs in this range is

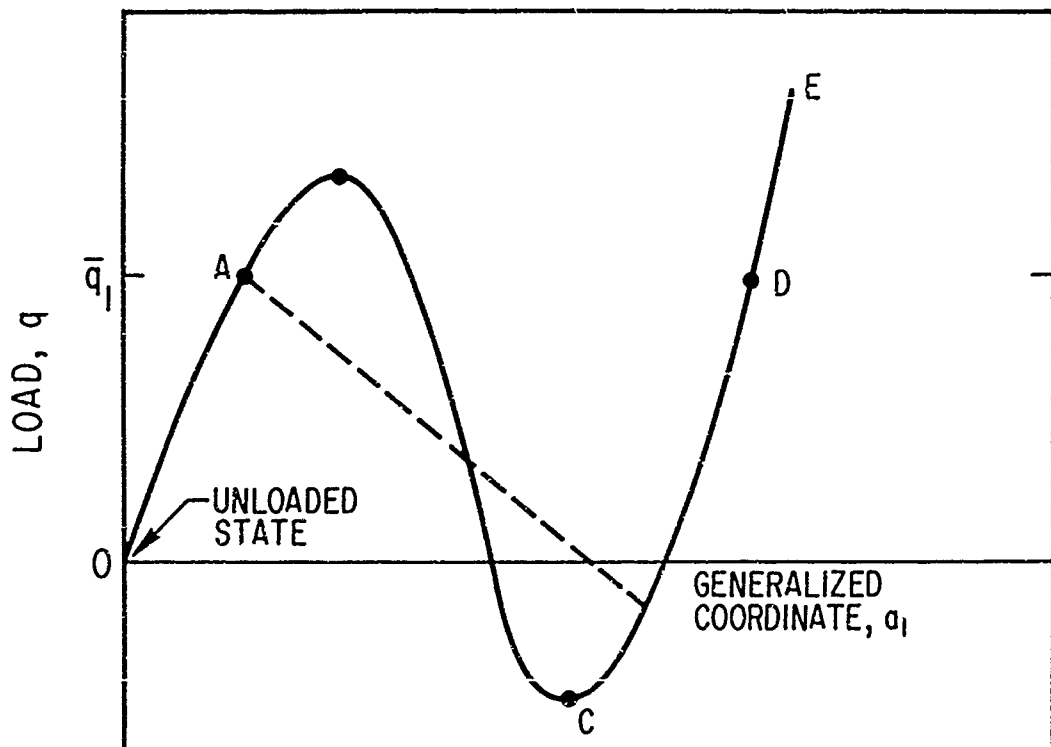
$$\bar{q}_1 = \frac{e + (e^2 - 4)^{3/4}}{6\sqrt{3}} \quad (3)$$

$2 < e \leq \sqrt{22}$

For $e > \sqrt{22}$, the arch becomes unstable with respect to infinitesimal perturbations in the nonsymmetric mode at the intersection of the symmetric and nonsymmetric equilibrium states (i.e., at the bifurcation point A in Figure 3b). Again the arch snaps through and vibrates about a large deflection equilibrium state (point D in Figure 3b). Since this phenomenon involves a bifurcation point and both the symmetric and nonsymmetric modes of the system, it is



a. TYPICAL LOAD DEFLECTION CURVE: $2 < e < 4.69$



b. TYPICAL LOAD DEFLECTION CURVES: $e > 4.69$

Figure 3. Static Load Deflection Curves for Shallow Arch

referred to as "snap-buckling." The critical value of the load parameter for instability in this range is

$$\bar{q}_1 = e + 3(e^2 - 16)^{1/2} \quad (4)$$

$$e > \sqrt{22}$$

Since the critical instability loads of Eqs. 3 and 4 also correspond to the occurrence of large deflections, they are considered to be the critical static loads for the system.

2.2 CIRCULAR RING

In the ring example the external pressure load is uniform. The radial and angular displacement components of the middle surface of the ring (see Figure 1b) are described by

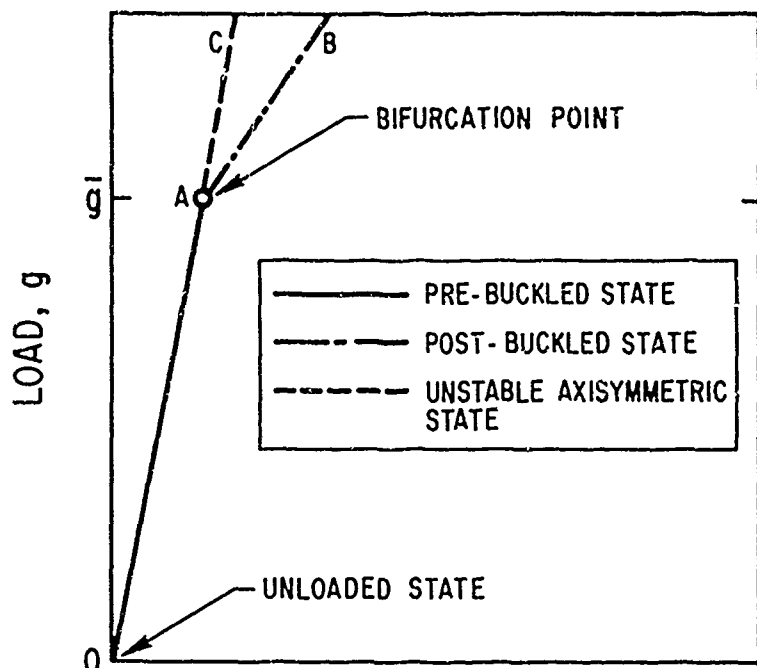
$$\zeta(\theta) = r_o + r_m \sin m\theta \quad (5a)$$

$$\psi(\theta) = c_m \cos m\theta \quad (m = 2, 3, 4, \dots) \quad (5b)$$

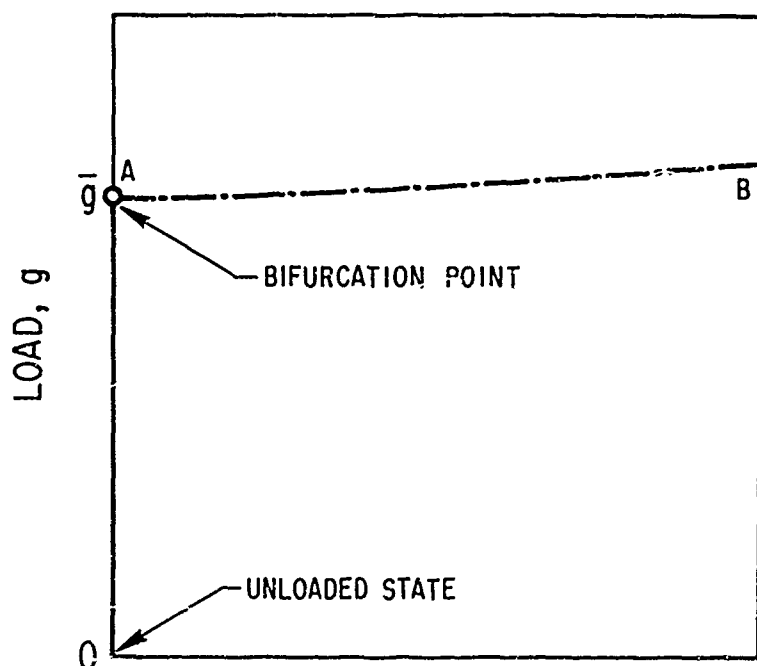
where r_o denotes the axisymmetric component of the radial displacement and r_m and c_m describe the nonsymmetric component of the displacement.

Eqs. 5a and 5b satisfy the condition that the displacement be continuous and periodic around the circumference of the ring. The generalized coordinates r_o , r_m , and c_m are governed by a set of coupled nonlinear algebraic equations. The solution of these equations determines the static load deflection characteristics of the ring.

An example of these characteristics is shown in Figures 4a and 4b, which respectively illustrate the axisymmetric and nonsymmetric components of the radial displacement. The load deflection curves of the ring are seen to



a. AXISYMMETRIC DISPLACEMENT



b. NONSYMMETRIC DISPLACEMENT

Figure 4. Static Load Deflection
Curves for Circular Ring

exhibit a bifurcation point at a specific level of the pressure load (point A in Figures 4a and 4b). For loads that are lower than this level, the equilibrium states are axisymmetric (i.e., $r_o \neq 0$, $r_m = 0$, $c_m = 0$); whereas, for loads that are higher than the bifurcation load, both axisymmetric equilibrium states and nonsymmetric equilibrium states (i.e. $r_o \neq 0$, $r_m \neq 0$, $c_m \neq 0$) can co-exist. An infinitesimal stability analysis of the axisymmetric equilibrium states (path OC in Figure 4a) reveals that they become unstable with respect to nonsymmetric perturbations at the appropriate bifurcation points. The most critical case is associated with the fundamental nonsymmetric mode of deformation (i.e., for $m = 2$). The bifurcation point and loss of stability for this case occur at the following value of the load parameter g :

$$\bar{g} = \frac{1}{4} \left(\frac{h}{R} \right)^2 \quad (6)$$

where h and R denote the thickness and radius of the ring, respectively. For $g > \bar{g}$, the ring adopts a stable nonsymmetric equilibrium state (branch AB in Figures 4a and 4b). The phenomenon in this case involves a bifurcation point but does not involve snapping. It is referred to as "buckling," and the post-critical stable nonsymmetric equilibrium states are referred to as post-buckled equilibrium states. It will be noted in this case that the appearance of instability corresponds to a significant loss in the stiffness of the structure (see Figure 4). Thus, the critical instability load given by Eq. 6 can be treated as the critical static load for the ring structure.

2.3 FINAL REMARK

The essential difference between the buckling and snapping systems lies in the existence or non-existence of stable equilibrium states adjacent to the initial equilibrium path for values of the load parameter slightly greater than the critical instability load. If such states do not exist, the system snaps with increase of load. If they do exist, the structure suffers a loss of stiffness, the severity of this loss depending upon the particular buckling system.

3. DYNAMIC LOAD PROBLEM

This section explores the behavior of the buckling and snapping systems when they are subjected to selected dynamic loading. The response of either system is determined by numerical integration of the governing nonlinear equations of motion.* The critical dynamic loads are directly defined upon the basis of this response; the infinitesimal stability analysis is dispensed with in this case, since a previous investigation by the author (Reference 6) demonstrated that the critical dynamic loads determined from infinitesimal stability considerations are not necessarily of practical significance.**

3.1 SHALLOW ARCH

The transverse position $\eta(\xi, \tau)$ of the arch is represented by Eq. 2 where the generalized coordinates a_1 and a_2 are now functions of time. The nonlinear differential equations governing these generalized coordinates are of the form

$$\frac{d^2 a_1}{d\tau^2} + \gamma \frac{da_1}{d\tau} + \omega_1^2 a_1 + F_1(a_1, a_2) + q_1(\tau) = 0 \quad (7)$$

$$\frac{d^2 a_2}{d\tau^2} + \gamma \frac{da_2}{d\tau} + \omega_2^2 a_2 + a_2 F_2(a_1, a_2) = 0 \quad (8)$$

where γ denotes a viscous damping coefficient. The constants ω_1 and ω_2 are proportional to the free vibration frequencies of the fundamental

*The partial differential equations governing the elastic response of the two systems are presented for reference in the Appendix; a detailed development of these equations can be found in References 6 and 8.

**This lack of significance arises because the growth of the unstable motions can be rapidly suppressed by nonlinear terms that are typically neglected in an infinitesimal stability analysis. Thus, unstable infinitesimal motions produced by a dynamic loading do not necessarily develop into large amplitude responses.

symmetric and nonsymmetric modes, respectively; the terms $F_1(a_1, a_2)$ and $F_2(a_1, a_2)$ are nonlinear coupling terms.

It will be noted that the symmetric mode is directly excited by the external load (see the inhomogeneous term $q_1(\tau)$ in Eq. 7). The nonsymmetric mode response is parametrically excited by the response in the symmetric mode by means of the term $F_2(a_1, a_2)$ in Eq. 3. Again we consider the behavior of the arch for $q \geq 0$ and $2 < e \leq 20$. The response to a given time-dependent pressure load is obtained by numerical integration of Eqs. 7 and 8, the integration scheme employed being a variable step size, fifth order, predictor-corrector method (Reference 9).

The procedure followed consists of fixing the load duration and obtaining the response at successively higher values of the load parameter. For most of the range of interest, i. e., the range $q \geq 0$ and $2 < e \leq 20$, the maximum level of this response is found to exhibit a distinct jump at a particular level of the load (an example of this behavior is shown in Figure 5 for the case of a step loading, i. e., $\tau_d = \infty$). The appearance of this jump corresponds to the development of a response that encompasses a snapped equilibrium state of the system* (see Figure 5). This response is considered as constituting dynamic elastic snapping. The critical dynamic load for snapping is then the lowest load required to produce such a response. This criterion can be applied over the complete range of pulse loads (i. e., between the impulse and step load limits) for those arch geometries that possess snapped equilibrium states for $q_1 \geq 0$.

If the system does not possess a snapped equilibrium state for $q_1 = 0$, it may be necessary to introduce another criterion in order to define a critical impulsive load. A possible procedure for employment in such a case would consist of imposing a maximum stress limitation and basing the critical load upon this criterion. This is the procedure that is adopted later for the problem of

* This equilibrium state can be the snapped equilibrium state corresponding to the specified load level q_1 or the snapped equilibrium state corresponding to $q_1 = 0$. The first case is appropriate for long duration loads, while the second case is appropriate for short duration impulsive loads.

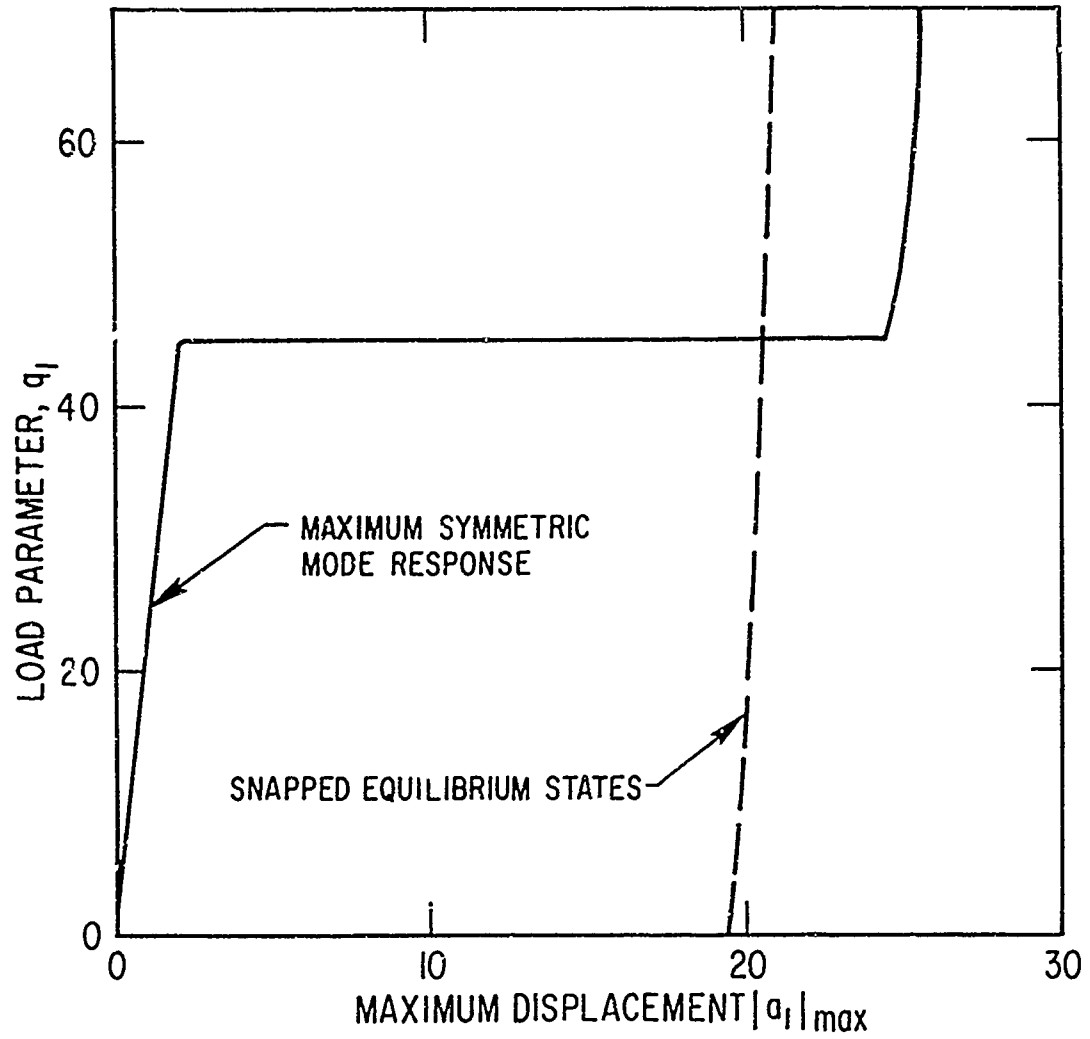


Figure 5. Variation of $|a_1|_{\max}$ with Load Parameter: $c = 10$

the circular ring subjected to an impulsive load. However, since the initial criterion suffices for most of the specified range of arch geometries,^{*} we will defer discussion of alternate criteria until later.

Employing the initial criterion, we obtain critical dynamic loads for a variety of arch geometries and load conditions.^{**} An example of the variation of the critical load with arch geometry is shown in Figure 6 for the case of a step load and zero damping. The results are presented in terms of the critical load ratio q_1^*/\bar{q}_1 and the geometric parameter e . Examining this figure, we note that the critical dynamic loads q_1^* are less than the corresponding critical static loads \bar{q}_1 for the range $2 < e < 8.6$, and that they are greater than the critical static loads for $e > 8.6$. These latter "superstatic" step loads are reduced to the level of the critical static loads by the presence of small damping (Reference 6); on the other hand, the "substatic" loads are increased by the presence of damping.

The response of the arch under a supercritical step load is found to be primarily in the symmetric mode $a_1(\tau) \sin \xi$ for the range $2 < e < 4.5$. An example of this type of response is shown in Figure 7. The behavior of the arch in this range is essentially a single degree of freedom phenomenon and is adequately described by the symmetric mode response. This type of dynamic snapping is referred to as "direct" snapping (Reference 6). For $e > 4.5$, the mechanism of snapping involves a complicated interaction between the symmetric and nonsymmetric mode response. This interaction consists of the parametric excitation of the nonsymmetric mode by the initial response in the symmetric mode followed by the interaction of this excited response back with the symmetric mode. An example of this type of response is shown in Figure 8. From the figure we see that the nonsymmetric mode response grows under the parametric excitation supplied by the symmetric mode, and.

^{*}The criterion based upon a response encompassing a snapped equilibrium state can be applied for $e \geq 4$. At lower values of e the specified type of arch does not possess a snapped equilibrium state at $q_1 = 0$.

^{**}An equivalent jump criterion has been employed in References 10-13.

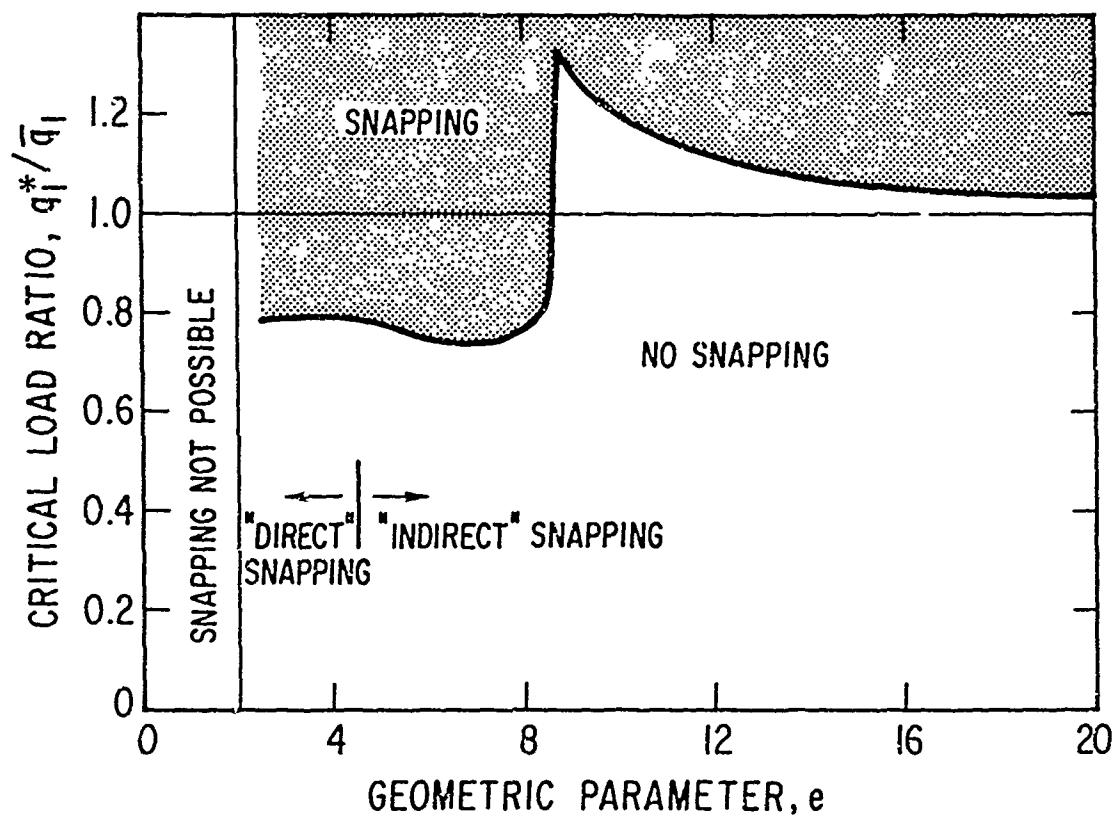


Figure 6. Variation of Critical Step Load with Arch Geometry

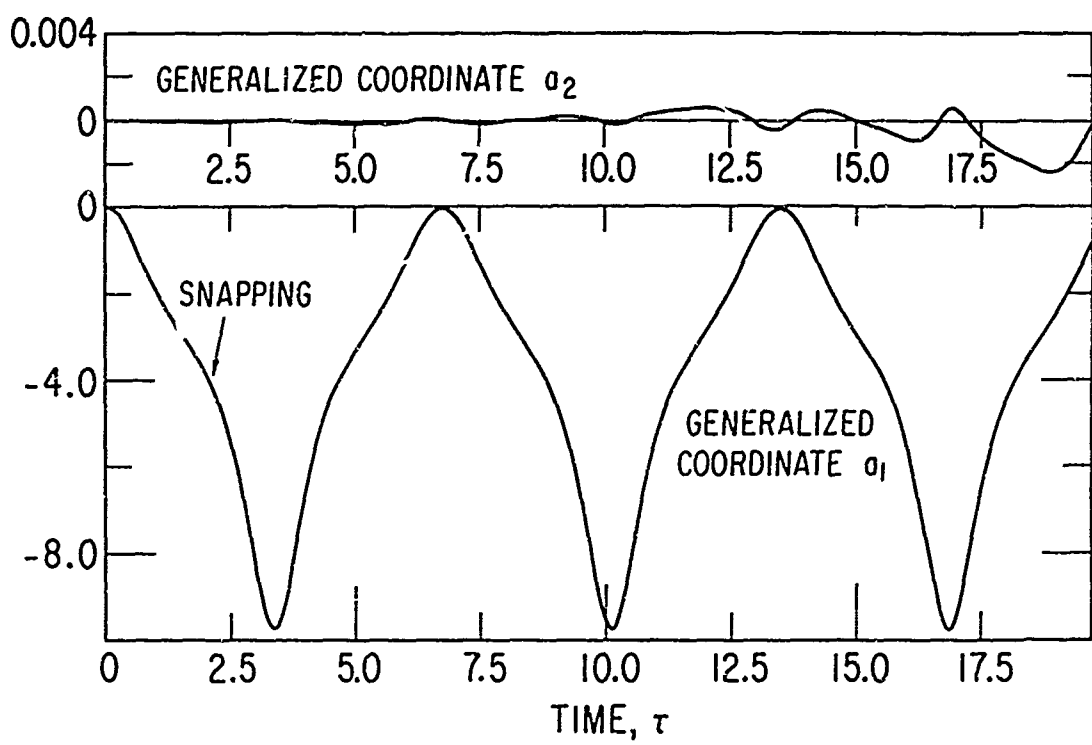


Figure 7. Response of Arch to Supercritical Step Load: $e = 4$

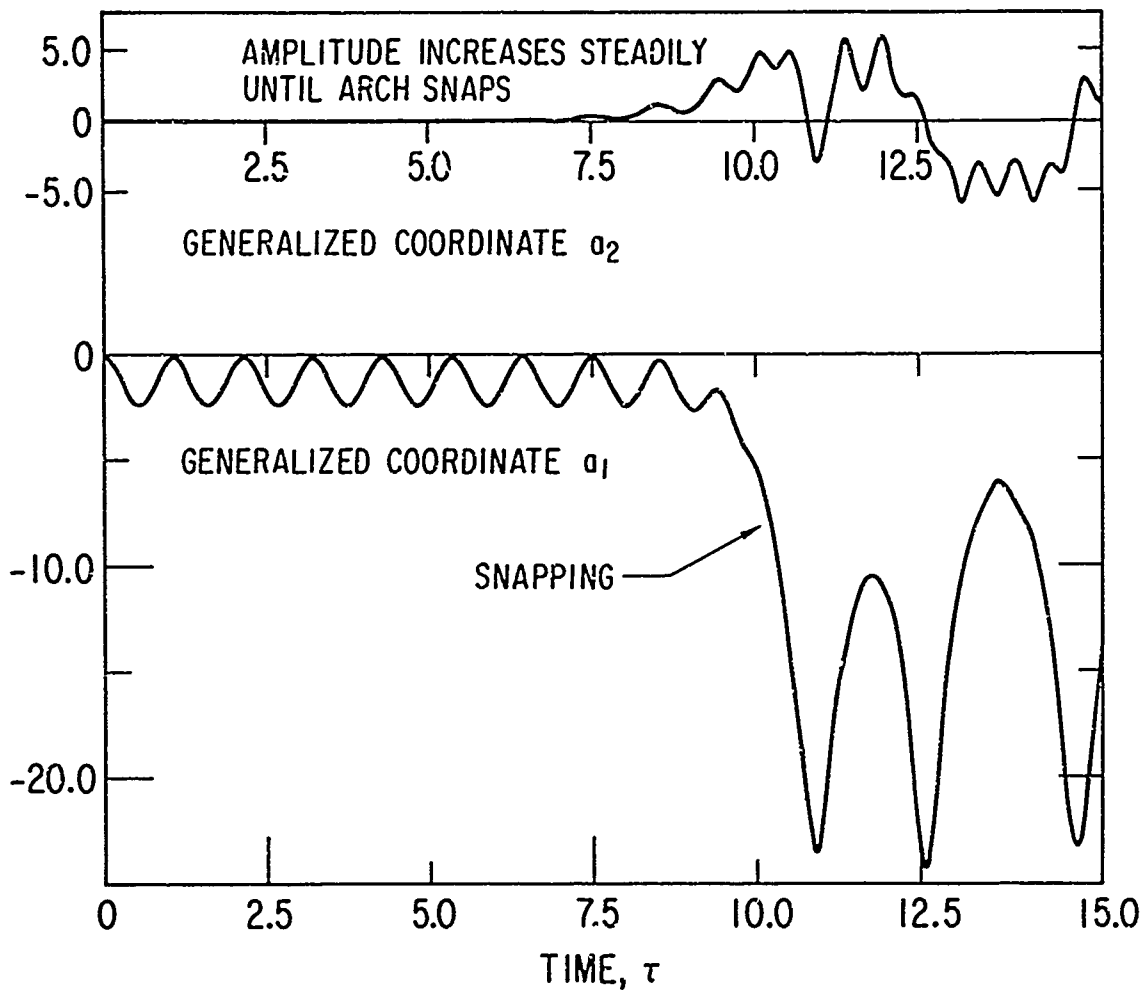


Figure 8. Response of Arch to Supercritical Step Load: $e = 10$

unlike the direct snapping mechanism, the arch vibrates for a number of cycles prior to snapping. The phenomenon in this case is referred to as "indirect" or "parametrically induced" snapping (Reference 6).*

The important difference between this mechanism and the direct snapping phenomenon is the essential role played by the nonsymmetric mode response.

The effect of load duration on the critical load level is illustrated in Figure 9 for two arch geometries. These geometries ($e = 4$ and $e = 7$) were selected to represent cases where the snapping phenomenon is controlled by the direct and indirect snapping mechanisms, respectively. The results are presented in terms of the critical load ratio $\frac{q_1^*}{\bar{q}_1}$ and the ratio τ_d/τ_1 , where τ_1 denotes the period of the fundamental symmetric mode. We note that the general features of the two critical load curves are the same: namely, an increase in critical load ratio with decrease in the load duration ratio. The difference in the detailed behavior of the load curves is due to the different mechanisms of snapping. This detailed behavior depends quite strongly upon the particular arch geometry.

When the ratio τ_d/τ_1 becomes sufficiently small, the impulse imparted to the structure rather than the load level becomes the most significant load parameter. The critical values of the impulse parameter I are shown as functions of τ_d/τ_1 in the inset of Figure 9. The variation of the critical impulse parameter with the geometric parameter is shown in Figure 10 for the limiting case of $\tau_d/\tau_1 \rightarrow 0$.

*The need to satisfy the conditions of parametric resonance as a prerequisite for the occurrence of this mechanism has been employed (Reference 6) to explain the character of the critical step load curves for $e > 4.5$.

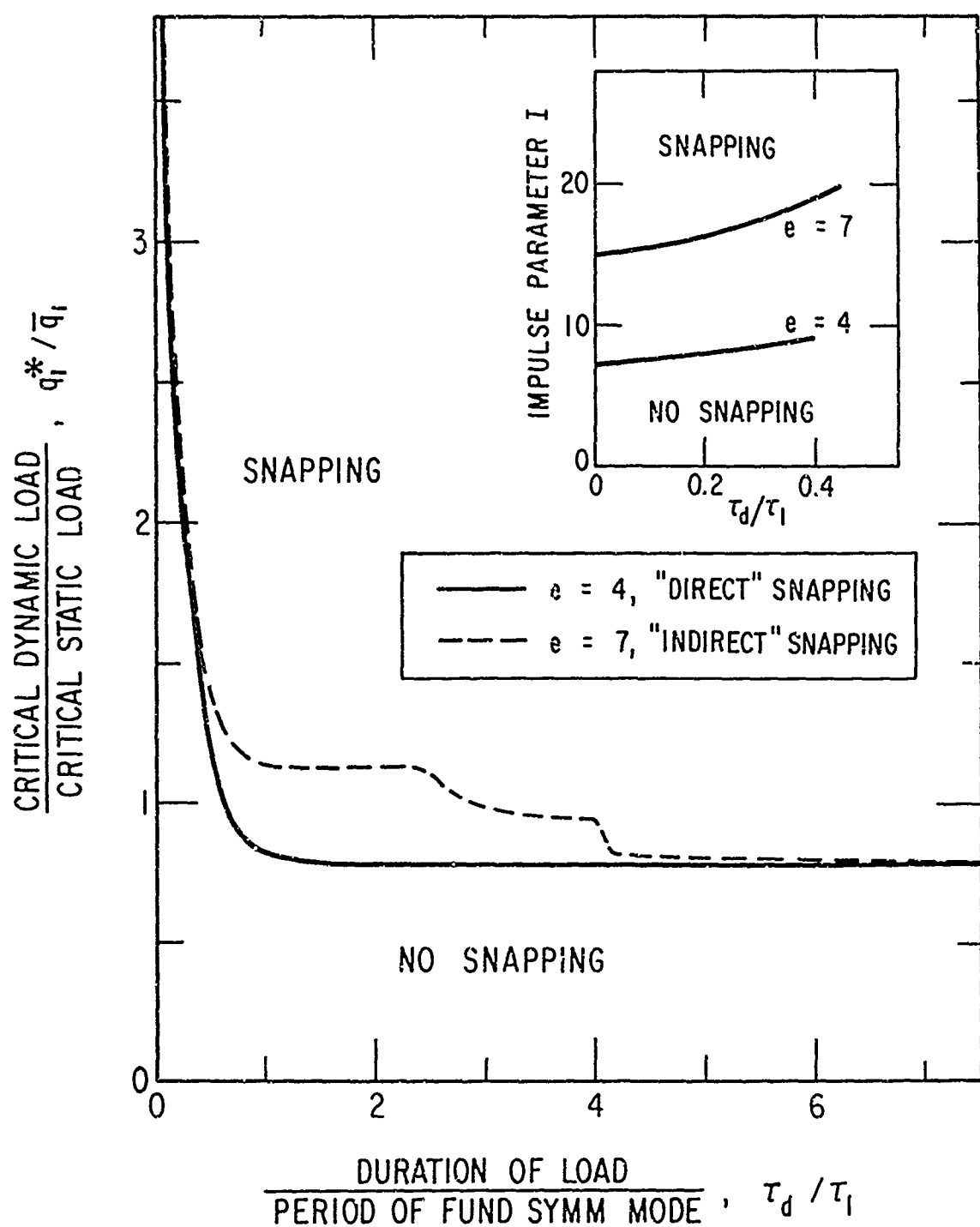


Figure 9. Variation of Critical Load Ratio
with Load Duration

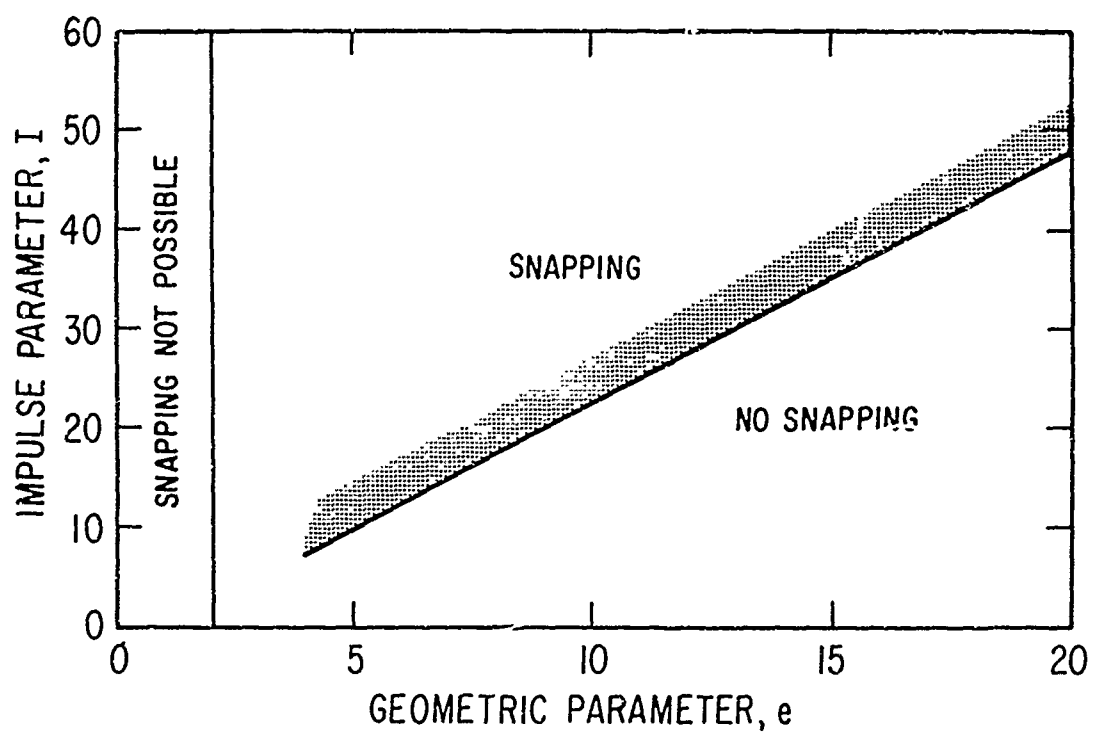


Figure 10. Variation of Critical Impulse Parameter
with Arch Geometry

The almost linear character of this variation is related to two facts:

- a. The minimum amount of kinetic energy input required to surmount the potential "barrier" between the unloaded and snapped equilibrium states of the arch is almost proportional to the square of the geometric parameter e .
- b. Satisfaction of the conditions of parametric resonance enables the system to pass over into the snapped state at such energy input levels.

It should be noted in passing that the linear variation does not persist at somewhat higher values of e , since the parametric resonance conditions are not satisfied at the foregoing minimum required impulse levels. Thus, impulse levels higher than this minimum are required to produce snapping of such arch geometries.

3.2 CIRCULAR RING

The radial and circumferential displacement components of the ring are again represented by Eqs. 5a and 5b, where the generalized coordinates are now treated as functions of time. The coordinates are governed by a set of coupled nonlinear ordinary differential equations whose form is similar to Eqs. 7 and 8. The axisymmetric mode response $r_0(\tau)$ is directly excited by the loading. The nonsymmetric mode response is parametrically excited by the axisymmetric response. The behavior of the ring is determined by numerical integration of the nonlinear equations of motion. The numerical method and procedure followed are similar to those employed in the problem of the shallow arch.

An example of the variation (with load level) of the maximum radial displacement in a nonsymmetric mode is presented in Figure 11 for the case of a step loading ($\tau_d = \infty$). Although the results are presented for a specific nonsymmetric mode ($m = 5$), the important features are representative of the results obtained for other nonsymmetric modes.* From the figure we see that the

*A detailed study of the nonlinear response of a circular ring under a step pressure loading can be found in Reference 8.

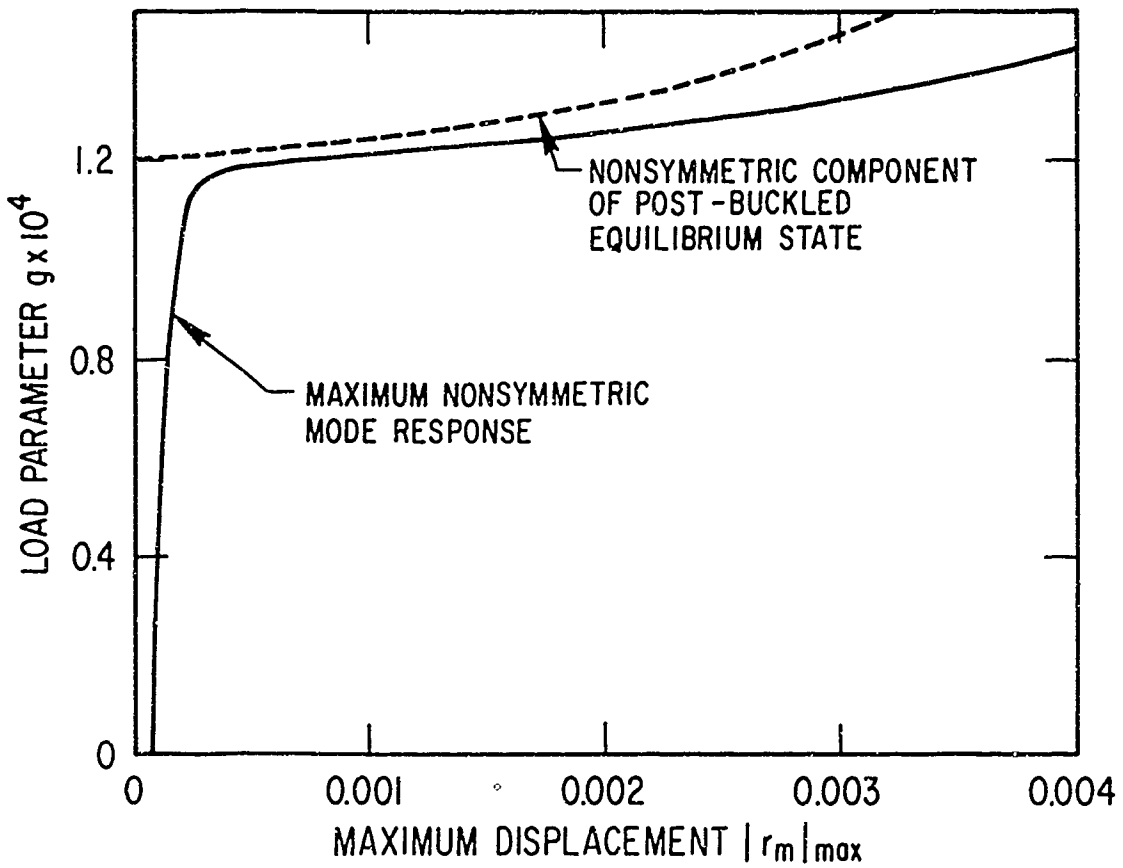


Figure 11. Variation of r_m max with Load Parameter:
 $R/h = 129, m = 5$

response level exhibits a rapid growth above a particular value of the load. The appearance of this growth corresponds to the development of a response that encompasses the corresponding post-buckled equilibrium state of the ring (see Figure 11). Such a response is considered as constituting dynamic elastic buckling. The critical load for dynamic elastic buckling is then the lowest load required to produce this type of response. This criterion is employed to determine the critical values of the step load for the range $10 < R/h < 1300$. These critical step loads are found to be associated with the fundamental nonsymmetric mode. Their levels are essentially identical to the corresponding critical static buckling loads. Thus,

$$g^* \approx \frac{1}{4} \left(\frac{h}{R} \right)^2 \quad (9)$$

$(\tau_d = \infty)$

An example of the response of the ring to a supercritical step load is shown in Figure 12. The important interaction between the modes excited under this loading is the parametric excitation of the nonsymmetric mode by the response in the axisymmetric mode.

We find that this interaction is the important response mechanism when the ring is subjected to an impulsive pressure load (i.e., $\tau_d/\tau_o \ll 1$, where τ_o denotes the period of the axisymmetric mode). However, in this case the maximum response level does not exhibit any distinctive regions of rapid growth that would serve to distinguish a critical value of the dynamic load. An example of this type of behavior is illustrated in Figure 13. The variation of the response level in this figure should be compared with that shown in Figures 5 and 11.

In the absence of such distinguishing features in the elastic response problem, we introduce the idea of plastic deformation and hypothesize the following "failure" mechanism: namely that the ring may be considered to have "failed" if the bending stresses developed in the response result in the formation of

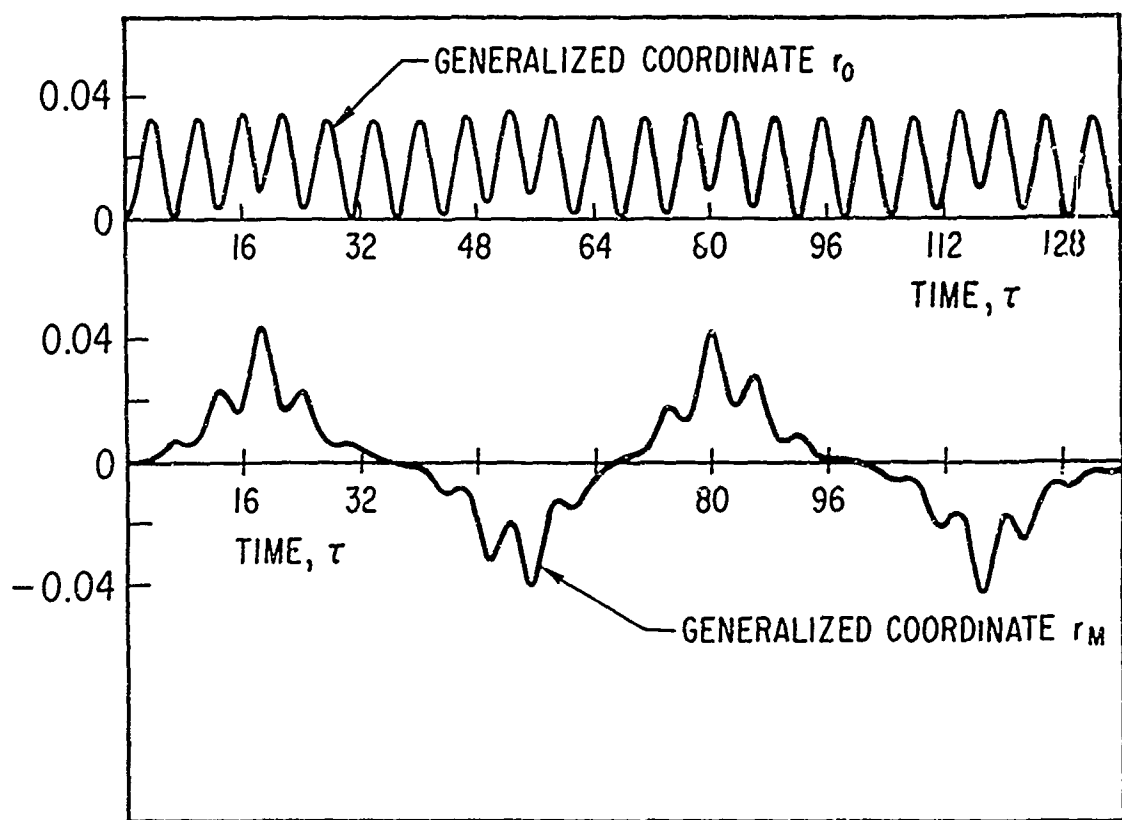


Figure 12. Response of Circular Ring to Step Load:
 $R/h = 12.9$, $m = 5$

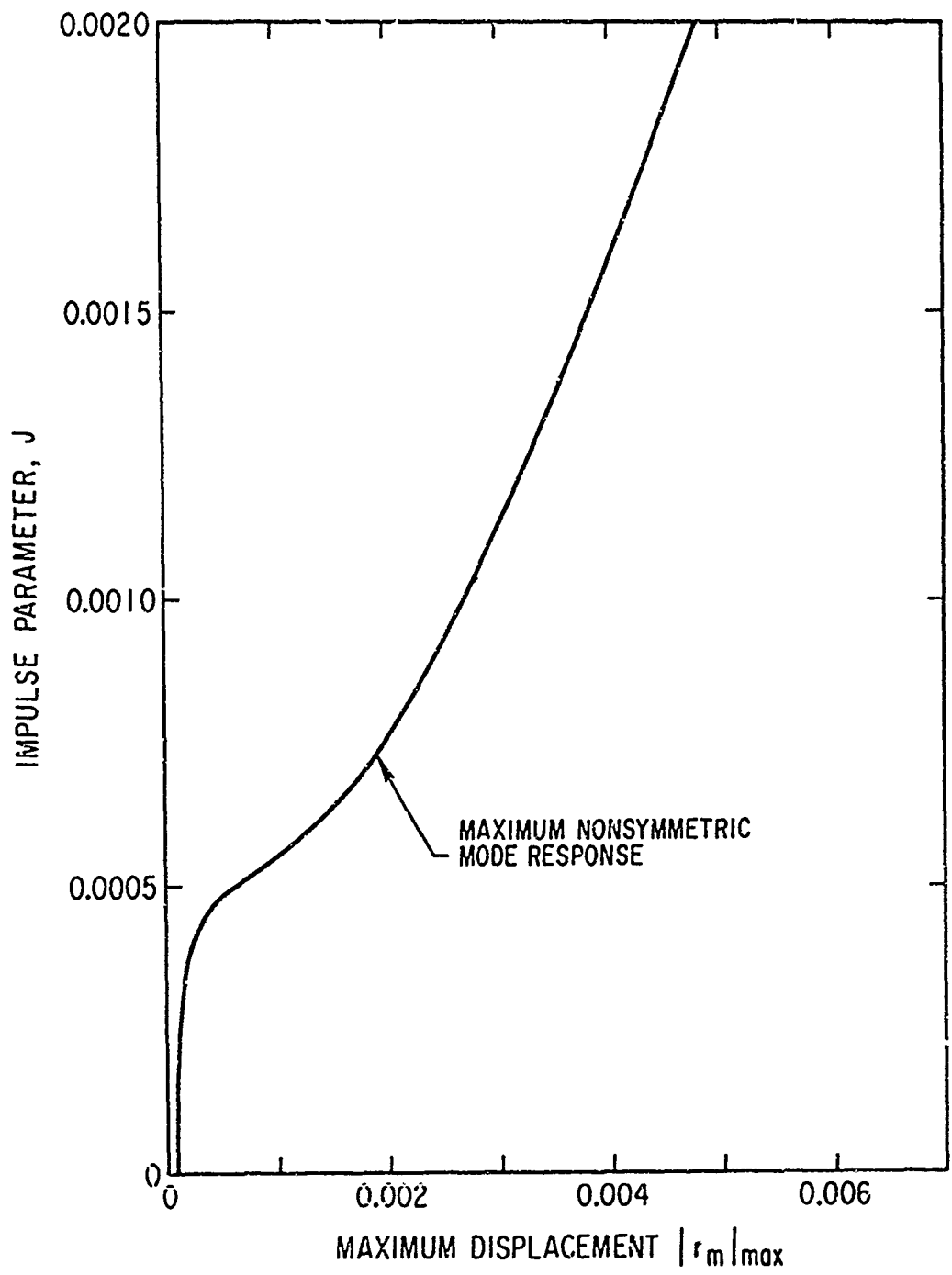


Figure 13. Variation of $|r_m|_{\max}$ with Impulse Level:
 $R/h = 129, m = 15$

plastic hinges. However, rather than analyze the extremely complicated elastic-plastic response problem, we take a conservative approach and consider that the system is critical when the maximum elastic stress just equals the yield stress of the material. Thus, the critical impulsive load is the lowest impulsive load required to produce such a stress level. We will refer to this phenomenon as dynamic elastic-plastic buckling.

An example of the critical impulse levels determined with the use of this definition is shown in Figure 14. The results are presented in terms of the impulse parameter J and the geometric parameter R/h . These results are obtained for the case of σ_y/E equal to 0.004, where σ_y denotes the yield stress and E represents Young's modulus of the material. The mode numbers m of the associated critical nonsymmetric modes are also presented in Figure 14. It will be noted that, unlike the step load problem, the critical response under impulsive loads involves the higher nonsymmetric modes of the system.

Finally, we illustrate the effect of load duration on critical load levels in Figure 15. The results are obtained for R/h equal to 129 and are presented in terms of the ratios g^*/\bar{g} and τ_d/τ_o . The critical load curve exhibits the same general feature that was noted in the case of the arch: an increase in critical load level with decrease in load duration. However, the curve in this case is composed of two distinct branches, these branches corresponding to the phenomena of dynamic elastic and dynamic elastic-plastic buckling.

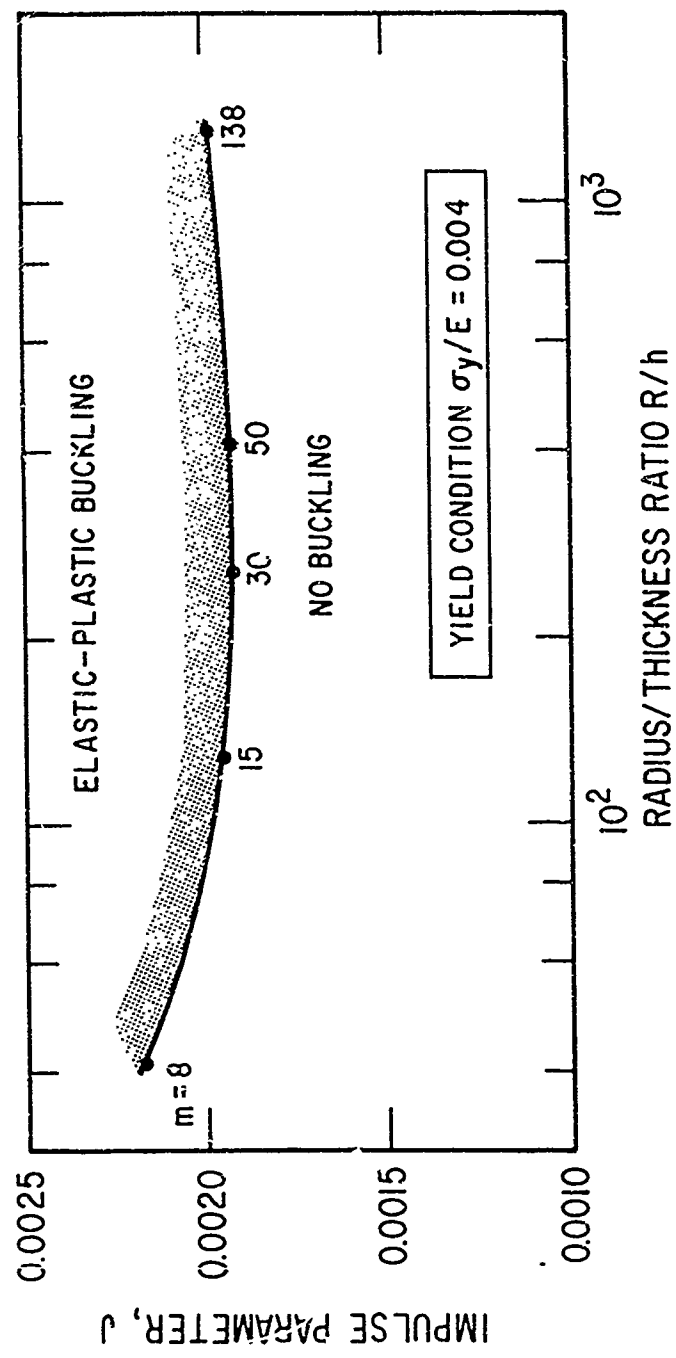


Figure 14. Variation of Critical Impulse Parameter with Ring Geometry

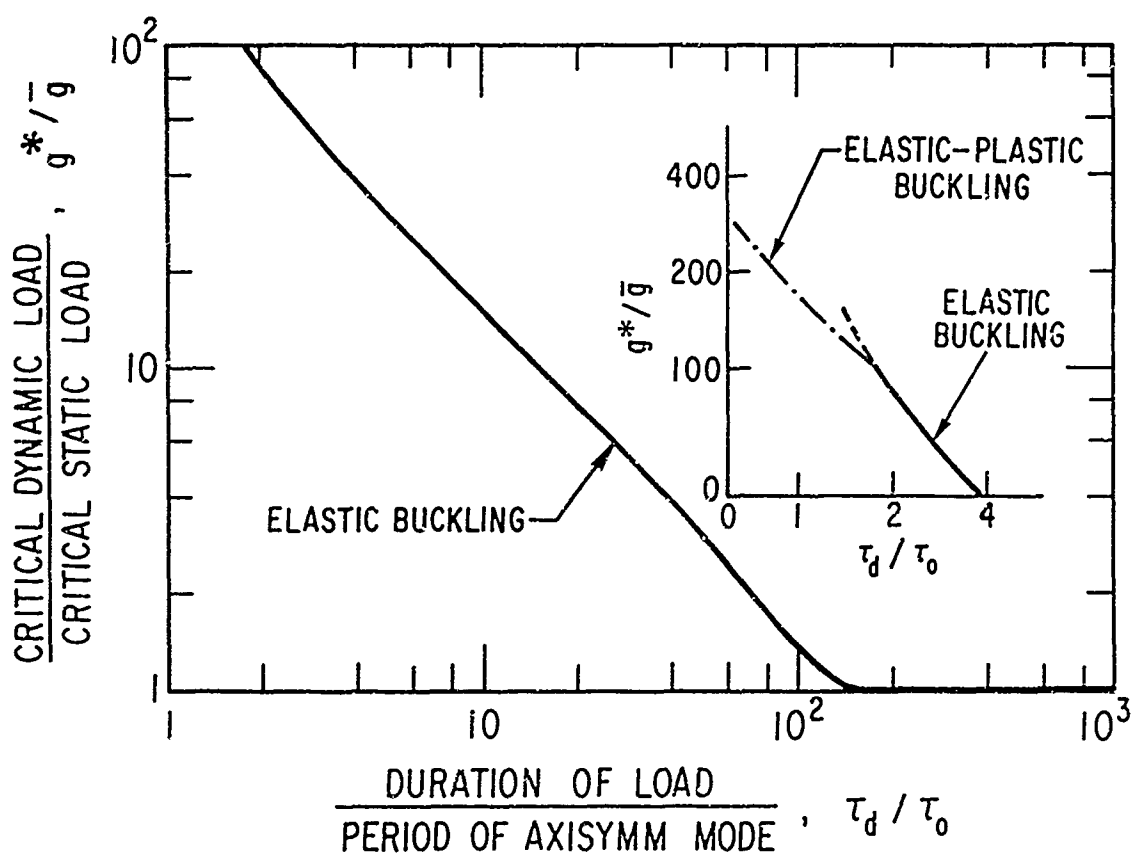


Figure 15. Typical Variation of Critical Load Ratio
with Load Duration: $R/h = 129$

4. COMPARISON OF CRITICAL LOADS

In the preceding section we have described the behavior of our two sample systems under the specified type of dynamic loading. We will now see how the critical dynamic loads compare with the corresponding critical static loads. This comparison may best be made by examining Figures 9 and 15. These figures illustrate the dependence of the ratio of the critical dynamic and static loads upon the ratios τ_d/τ_1 and τ_d/τ_o for the shallow arch and circular ring. In both cases we see that the most critical dynamic load conditions (i.e., conditions for the lowest value of the critical load ratio) correspond to the case of a step load. However, there is an important difference between the two systems: the minimum value of the critical load ratio is appreciably less than unity in the case of the arch (about 0.78 for the cases shown in Figure 9), whereas it is equal to unity in the case of the ring.

Thus, particular arch geometries can exhibit dynamic weakening (i.e., collapse at dynamic loads that are lower than the corresponding critical static loads) if the load duration is sufficiently long. As a corollary to this we see that the design of such systems against dynamic loads, if based upon the critical static load, would prove to be unconservative. The load duration required to produce such dynamic weakening, as measured by the ratio τ_d/τ_1 , depends strongly upon the type of mechanism controlling the snapping process. This may be seen by comparing the two curves shown in Figure 9. There we see that the critical load ratios are less than unity if $\tau_d/\tau_1 > 0.6$ in the case of direct snapping, and if $\tau_d/\tau_1 > 2.8$ for the case of indirect snapping.* As the ratios τ_d/τ_1 and τ_d/τ_o are reduced, the critical load ratios increase and the systems are able to withstand dynamic pressure loads that are substantially in excess of the critical static pressures. Thus, static design in such cases would be highly conservative.

*We should also note that some "indirect" snapping geometries do not exhibit dynamic weakening (see discussion of shallow arch problem in Section 3).

5. COMPARISON WITH RELATED WORK

It is of interest to compare the present work with related studies in this field. This comparison will illustrate the diversity of problems arising when the external loading is time-dependent.* Let us first consider buckling systems. In this category we have studies of the buckling of elastic columns under axial impact loads (References 19-28), of the response of plates to in-plane compressive loads (Reference 29), and of the buckling of rings and cylinders under external pressure loads (References 30-33).

The studies of the column problem can be divided roughly into three categories:

- a. Analyses that include the effect of axial inertial forces and consider the propagation of the loading pulse in the column (References 19-22)
- b. Investigations that neglect the axial inertial forces and determine the modes that are most highly excited by intense impulsive loads (References 23-25)
- c. Studies that neglect the axial inertial forces and determine the response of initially imperfect structures to the specified dynamic load (References 24, 26-28)

With the exception of Reference 28, the studies in Categories (b) and (c) are based upon linear equations of motion, as are the earlier investigations in the first category (References 19 and 20). The investigation of the plate problem (Reference 29) also employs linear equations and falls within the third category of analysis. References 30 and 31 study the response of cylindrical shells to external pressure loads and are based upon nonlinear

* We limit ourselves to the pulse type of time-dependent load considered in the present paper. Studies of the dynamic response produced by specified motion of structural boundaries or by loads that increase linearly with time can be found in References 14-17, while a comprehensive discussion of dynamic instability under periodic loading will be found in Reference 18.

equations of motion. References 32 and 33 are linear analyses and are concerned with the determination of the modes (of an infinitely long cylinder or ring) which are most highly excited by intense impulsive pressure load. These latter studies are similar to those in the second category of analysis mentioned previously.

Of the various studies described above, the works of References 30 and 31 are most similar to the buckling part of the present study. However, they are of considerably less scope and only one of the investigations (Reference 30) specifically considers the question of critical dynamic load.* The other investigations treat particular aspects of the dynamic load problem (stress wave propagation, mode excitation, imperfect system response, etc.). The stress wave studies are appropriate to problems where the load duration is comparable to the time required for a stress wave to traverse the system. In the present study, stress wave effects are not expected to be significant since the transit path simply consists of the thickness of the structure. The mode excitation studies have been used to explain the character of the post-buckled deformation shapes produced by impulsive load. However, they have a disadvantage in that they do not treat the practically important question of critical load determination. The studies of the dynamic response of initially imperfect structures can be considered as the dynamic load analogue of the deformation analyses performed for initially imperfect structures subject to the corresponding static loads.** As such, these studies can be considered as being complementary to the type of analysis carried out in the present investigation.

* Reference 30 introduces a safe load based upon the total stress at any point in the structure not exceeding the ultimate strength of the material.

** The analysis of a perfect system subject to a static load generally results in a stability or eigenvalue problem; however, if the system is considered to be initially imperfect the analysis reduces to a deformation study (For example, compare the analysis of perfectly straight and initially curved struts subject to axial load).

Now let us consider the investigations that treat snapping systems. In this category we have the snapping of shallow domes, cones, curved panels, and shallow arches under external pressure loads (References 10-13, 34-40) and the snapping of circular cylinders under dynamic axial load (References 41-43). A combined load problem involving the snapping of axially loaded cylinders under dynamic lateral pressure loads is treated in References 42 and 44.

With the exception of References 41 and 43, these studies are based upon non-linear equations of motion and are primarily concerned with determining the structural response to the specified dynamic loading. This response is then employed to obtain the critical values of the dynamic load, the determination of these loads being effected with the use of a "jump" criterion that is equivalent to the response criterion employed in the present study of snapping systems.* These studies are clearly similar to the present analysis. However, a large number of the previous investigations (see References 10-13, 34-38) have been limited to the treatment of symmetric or axisymmetric types of deformation. As a result of this limitation, such investigations do not treat the indirect type of snapping phenomenon found to be important in the present study. Thus, the resulting critical dynamic loads could prove to be unrealistic for particular ranges of structural geometry.

A phenomenological theory for the dynamic buckling of a circular cylinder under axial impact load, including the effect of wave propagation, is presented in Reference 41. A linear analysis of mode excitation under dynamic axial load is given in Reference 43.

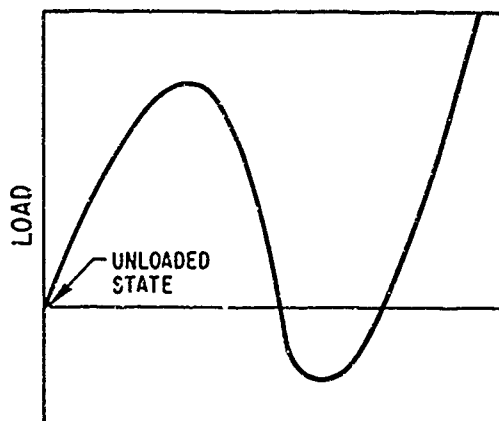
Finally, mention should be made of two investigations that are concerned with the use of simple models (Reference 45) and energy methods (Reference 46) for the estimation of critical dynamic loads.

* In some cases where the structure is analyzed as a single degree of freedom system, an equivalent energy criterion has been employed (see References 10, 13, and 37).

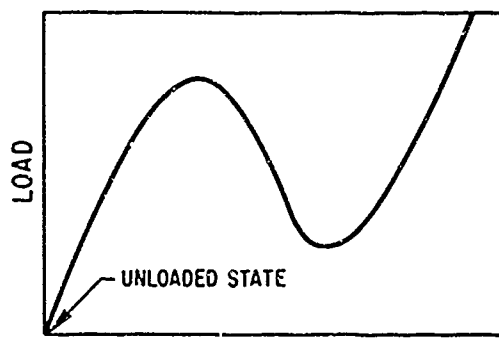
6. CONCLUDING REMARKS

This report has comprised a detailed study of the behavior under dynamic load of two particularly simple structural systems. The response of these systems was determined for wide ranges of the geometric and load parameters, and because of the simplicity of the systems it was possible in many instances to relate this response to the corresponding static load deflection characteristics of the structure. This relationship served as a basis for defining dynamic elastic snapping and dynamic elastic buckling. When such a relationship could not be established, the mechanism of dynamic elastic-plastic buckling was introduced. The specification of the phenomena was accompanied by the specification of the corresponding critical load criteria. Application of these criteria then led to the development of critical dynamic load data. The critical dynamic load criteria differed among themselves, and it was found that for some structural geometries different criteria had to be employed, depending upon whether the loading was impulsive or of long duration.

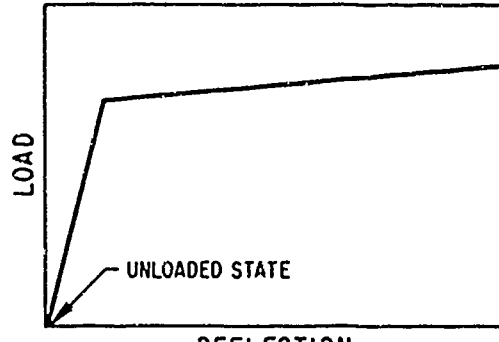
The different critical load criteria and their different application are intimately associated with the static load deflection characteristics of the structure. This aspect of the dynamic load problem suggests the development of a classification scheme for this type of problem. Such a scheme can be based upon the three types of static load deflection characteristics shown in Figure 16. The first two cases pertain to systems that exhibit snapping under a static load; these cases are labelled S. 1 and S. 2; they can be referred to as snapping systems. The distinction between them is based on their different behavior under the dynamic load. Considering $q \geq 0$, we see that the S. 1 system exhibits dynamic elastic snapping throughout the complete range of pulse loads. Thus, a single critical dynamic load criterion can be applied to this type of system. On the other hand, the S. 2 system exhibits dynamic elastic snapping for long duration loads and dynamic elastic plastic buckling for short duration impulsive loads. Two different critical load criteria are required for



DEFLECTION
a. SYSTEM S. 1



DEFLECTION
b. SYSTEM S. 2



DEFLECTION
c. SYSTEM B

Figure 16. Classification System

application over the range of pulse loads. The third case shown in Figure 16 corresponds to a system that exhibits buckling under a static load; this system is labelled B and can be referred to as a buckling system. Under a dynamic load it exhibits dynamic elastic buckling or dynamic elastic-plastic buckling, depending upon whether the loading is of long or short duration. Again, two different critical load criteria are required for the complete range of pulse loads.

This type of classification scheme should be applicable to other types of structural elements (e.g., domes, cylinders, columns) that are commonly encountered in elastic stability theory. The scheme should aid in the analysis of the behavior of these systems under dynamic loading. The nondimensional critical load data presented in Figures 9 and 15 should also serve as a guide in the design of elastic structures against this type of dynamic loading.

APPENDIX

PARTIAL DIFFERENTIAL EQUATIONS OF MOTION

The partial differential equations governing the behavior of the shallow arch and the circular ring are presented below for the purpose of reference. A detailed development of these equations can be found in References 6 and 8.

Shallow Arch

The nondimensional form of this equation is written (see Nomenclature for definitions) as

$$\frac{\partial^4 \eta}{\partial \xi^4} - \frac{d^4 \bar{\eta}}{d\xi^4} - \frac{1}{2\pi} \frac{\partial^2 \eta}{\partial \xi^2} \left(\int_0^\pi \left[\left(\frac{\partial \eta}{\partial \xi} \right)^2 - \left(\frac{d \bar{\eta}}{d \xi} \right)^2 \right] d\xi \right) + \gamma \frac{\partial \eta}{\partial \tau} + \frac{\partial^2 \eta}{\partial \tau^2} + q(\xi, \tau) = 0 \quad (A-1)$$

Where $\bar{\eta}(\xi)$ denotes the initial unstressed position of the arch,

$$\bar{\eta}(\xi) = e \sin \xi$$

The integral that appears in the third term of Eq. A-1 describes the stretching of the middle surface of the arch produced by the transverse displacement. The term $\gamma \partial \eta / \partial \tau$ represents a viscous damping force, this term being employed as a simple means of including the effect of damping in the analysis.

The function $\eta(\xi, \tau)$ is described by

$$\eta(\xi, \tau) = e \sin \xi + a_1(\tau) \sin \xi + a_2(\tau) \sin 2\xi \quad (A-2)$$

Substitution of this series into Eq. A-1 leads to a pair of coupled nonlinear equations governing the generalized coordinates $a_1(\tau)$ and $a_2(\tau)$.

Circular Ring

The deformation of the ring is based upon the assumptions of the Winkler theory of curved beams. The partial differential equations governing the radial displacement $\zeta(\theta, \tau)$ and the circumferential displacement $\psi(\theta, \tau)$ of the middle surface of the ring are

$$\frac{\partial^2 \zeta}{\partial \tau^2} + \gamma \frac{\partial \zeta}{\partial \tau} + \frac{1}{12} \left(\frac{h}{R} \right)^2 \left[\frac{\partial^4 \zeta}{\partial \theta^4} + 2 \frac{\partial^2 \zeta}{\partial \theta^2} + \zeta \right] - \epsilon_0 \left[1 + \frac{\partial \psi}{\partial \theta} - \zeta \right] \cdot \frac{\partial}{\partial \theta} \left[\epsilon_0 \left(\frac{\partial \zeta}{\partial \theta} + \psi \right) \right] = q \left(1 + \frac{\partial \psi}{\partial \theta} - \zeta \right) \quad (A-3)$$

$$\frac{\partial^2 \psi}{\partial \tau^2} - \frac{\partial}{\partial \theta} \left[\epsilon_0 \left(1 + \frac{\partial \psi}{\partial \theta} - \zeta \right) \right] + \epsilon_c \left(\frac{\partial \zeta}{\partial \theta} + \psi \right) = -q \left(\frac{\partial \zeta}{\partial \theta} + \psi \right) \quad (A-4)$$

and where ϵ_0 denotes the middle surface strain,

$$\epsilon_0 = \frac{\partial \psi}{\partial \theta} - \zeta + \frac{1}{2} \left(\frac{\partial \psi}{\partial \theta} - \zeta \right)^2 + \frac{1}{2} \left(\frac{\partial \zeta}{\partial \theta} + \psi \right)^2 \quad (A-5)$$

Again, a viscous damping term has been included in the equation as a simple means of incorporating the effect of damping. The displacement components are represented by the expressions

$$\begin{aligned} \zeta(\theta, \tau) &= r_o(\tau) + r_m(\tau) \sin m\theta \\ \psi(\theta, \tau) &= c_m(\tau) \cos m\theta \end{aligned} \quad (A-6)$$

Substitution of Eq. A-6 into Eqs. A-4 and A-5, followed by application of the Galerkin method, leads to a set of ordinary differential equations governing the generalized coordinates $r_o(\tau)$, $r_m(\tau)$, and $c_m(\tau)$.

DISCLAIMER NOTICE

**THIS DOCUMENT IS BEST QUALITY
PRACTICABLE. THE COPY FURNISHED
TO DTIC CONTAINED A SIGNIFICANT
NUMBER OF PAGES WHICH DO NOT
REPRODUCE LEGIBLY.**

OR are
Blank pg.
that have
been removed

**BEST
AVAILABLE COPY**

REFERENCES

1. S. P. Timoshenko and J. M. Gere, "Theory of Elastic Stability," McGraw-Hill, New York (1961)
2. A. E. H. Love, "The Mathematical Theory of Elasticity," Dover Publications, New York (1964)
3. W. A. Nash, "Recent Advances in the Buckling of Thin Shells," Applied Mechanics Reviews 13 (3), 161-164 (March 1960)
4. Y. C. Fung and E. E. Sechler, "Instability of Thin Elastic Shells," Proc. First Symp. on Naval Struct. Mech., 115-168, Pergamon Press, New York (1960)
5. H. J. Hoff and V. C. Bruce, "Dynamic Analysis of the Buckling of Laterally Loaded Flat Arches," J. Math. Phys. 32, 276-288 (1953)
6. M. H. Lock, "The Snapping of a Shallow Sinusoidal Arch under a Step Pressure Load," AIAA J. 4 (7), 1249-1256 (1966)
7. Y. C. Fung and A. Kaplan, "Buckling of Low Arches or Curved Beams of Small Curvature," NACA TN 2840, California Institute of Technology (1952)
8. M. H. Lock, "The Nonlinear Response of a Thin Circular Ring under a Uniform Step Pressure Load," Aerospace Corporation Report TR-1001 (2240-30)-1, El Segundo, California (1966)
9. W. E. Milne and R. R. Reynolds, "Fifth-order Methods for the Numerical Solution of Ordinary Differential Equations," J. Assoc. Comp. Mach. 9, 64-70 (1962)
10. J. S. Humphreys and S. R. Bodner, "A Criterion for Dynamic Buckling of Shallow Shells under Impulsive Loads," I. A. S. Paper 61-16, IAS 29th Annual Meeting, New York (1961)
11. P. P. Radkowski, J. S. Humphreys, R. G. Payton, S. R. Bodner, and B. Budiansky, "Studies on the Dynamic Response of Shell Structures and Materials to a Pressure Pulse," AFSWC-TR-61-31 (II), Avco Corp., Wilmington, Mass. (July 1961)
12. R. S. Roth, "Dynamic Instability of Shallow Spherical Shells Subjected to Pressure Pulse Loadings," RAD-TM-62-24, AVCO Corp., Wilmington, Mass. (May 1962)

13. J. S. Humphreys and S. R. Bodner, "Dynamic Buckling of Shells Under Impulsive Loading," J. Eng. Mech. Div., Am. Soc. Civil Engrgs. 88, (EM2) 17-36, (1962)
14. N. J. Hoff, "The Dynamics of the Buckling of Elastic Columns," J. Appl. Mech. 18, 68-74 (1951)
15. E. Sevin, "On The Elastic Bending of Columns due to Dynamic Axial Forces Including Effects of Axial Inertia," J. Appl. Mech. 27, 125-131 (1960)
16. A. S. Vol'mir, "On the Stability of Dynamically Loaded Cylindrical Shells," Soviet Physics-Doklady 3, 1287-1289 (1958)
17. V. L. Agamirov and A. S. Vol'mir, "Behavior of Cylindrical Shells under Dynamic Loading by Hydrostatic Pressure or by Axial Compression," Izv. Akad. Nauk. SSSR, Mech i Mashin., 3 (1959) English Translation by J. G. Adashko ARS J., 31, 98-101 (1961)
18. V. V. Bolotin, "The Dynamic Stability of Elastic Systems," translated by V. I. Weingarten, L. B. Greszczuk, K. N. Trirogoff, and K. D. Gallegos, Hoden-Day, San Francisco (1964)
19. G. Gerard and H. Becker, "Column Behavior under Conditions of Impact," J. Aero. Sci. 19, 58-60 (1952)
20. W. H. Hoppmann II, "Stability of a Prismatic Bar under the Influence of a Compressional Strain Wave," TR 7, Navy Contract NONR-248 (12), Johns Hopkins Univ. (1952)
21. N. J. Huffington, "Response of Elastic Columns to Axial Pulse Loading," AIAA J. 1 (9), 2099-2104 (1963)
22. A. S. Vol'mir and I. G. Kil'dibekov, "Buckling of Bars under Impact," Soviet Physics - Doklady 11 (4), 355-356 (1966)
23. M. A. Lavrent'ev and A. Yu. Ishlinskii, "Dynamic Forms of Loss of Stability of Elastic Systems," Dok. Adad. Nauk. USSR 64, 779-782 (1949). English Translation by R. M. Cooper in STL-TR-61-5110-41, Space Technology Laboratories, Los Angeles, California
24. G. W. Housner and W. K. Tso, "Dynamic Behavior of Supercritically Loaded Struts," J. Eng. Mech. Div., Proc. Amer. Soc. Civil Eng., 41-65 (1962)
25. H. E. Lindberg, "Impact Buckling of a Thin Bar," J. Appl. Mech. 32 (2), 315-322 (1965)
26. J. Taub and C. Koning, "Impact Buckling of Thin Bars in the Elastic Range Hinged at Both Ends," NACA TM 748 (1934)

27. J. H. Meier, "On the Dynamics of Elastic Buckling," J. Ae. Sc. 12, 443-440 (1945)
28. J. F. Davidson, "Buckling of Struts under Dynamic Loading," J. Mech. Phys. Solids, 2, 54-66 (1953)
29. G. A. Zizicas, "Dynamic Buckling of Thin Elastic Plates," J. Appl. Mech. 19, 1257-1266 (1952)
30. Y. I. Kadashevich and A. K. Pertsev, "Loss of Stability of a Cylindrical Shell under Dynamic Loads," Izv. Akad. Nauk SSSR, Mekh. i Mashin., 3 (1960). English Translation by K. N. Trirogoff and R. M. Cooper, ARS J. 32, 140-142 (1962)
31. C. W. Robinson, "Dynamic Buckling of an Elastically Supported Thin Cylindrical Shell under Dynamic Axial Load and Lateral Pressure," Sandia Corp. Report SCL-DR-65-28, Livermore, California (April 1965)
32. H. E. Lindberg, "Buckling of a Very Thin Cylindrical Shell Due to an Impulsive Pressure," J. Appl. Mech. 31 (2), 267-272 (1964)
33. W. Stuiver, "On the Buckling of Rings Subject to Impulsive Pressures," J. Appl. Mech. 32 (3), 511-518 (1965)
34. B. Budiansky and R. S. Roth, "Axisymmetric Dynamic Buckling of Clamped Shallow Spherical Shells," Collected Papers on Instability of Shell Structures - 1962, NASA TN D-1510, NASA Langley Research Center (December 1962)
35. R. R. Archer and C. G. Lange, "Nonlinear Dynamic Behavior of Shallow Spherical Shells," AIAA J. 3 (12), 2313-2317 (1965)
36. G. J. Simitses, "Dynamic Snap-through Buckling of Shallow Spherical Caps," AIAA/ASME 7th Structures and Materials Conference, Cocoa Beach, Florida (1966)
37. R. E. Fulton, "Dynamic Axisymmetric Buckling of Shallow Conical Shells Subjected to Impulsive Loads," J. App. Mech. 32 (1), 129-134 (1965)
38. B. E. Cummings, "Large Amplitude Vibration and Response of Curved Panels," AIAA J. 2 (4), 709-716 (1964)
39. P. T. Hsu and M. M. Chen, "Snapping Phenomena of Elasto-Plastic Curved Beams Under Static and Dynamic Loadings," Report AFOSR 2460, Mass. Inst. Tech. (January 1962)

40. J. S. Humphreys, "On Dynamic Snap-Buckling of Shallow Arches," AIAA J. 4 (6), 878-886 (1966)
41. A. P. Coppa, "The Buckling of Circular Cylindrical Shells Subject to Axial Impact," Collected Papers on Instability of Shell Structures - 1962, NASA TN D-1510, NASA Langley Research Center (December 1962)
42. R. S. Roth and J. M. Klosner, "Nonlinear Response of Cylindrical Shells Subjected to Dynamic Axial Loads," AIAA J. 2 (10), p. 788-1794 (1964)
43. H. E. Lindberg and R. E. Herbert, "Dynamic Buckling of a Thin Cylindrical Shell Under Axial Impact," J. Appl. Mech. 33 (1), p. 105-112 (1966)
44. L. R. Koval and J. P. O'Neill, "Stability of Axially Loaded Thin Cylindrical Shells Under Dynamic Lateral Pressures," Report EM 13-20, Space Technology Labs., Inc. (October 1963)
45. J. W. Hutchinson and B. Budiansky, "Dynamic Buckling Estimates," AIAA J. 4 (3), 525-530 (1966)
46. C. S. Hsu, "On Dynamic Stability of Elastic Bodies with Prescribed Initial Conditions," Int. Journ. Eng. Sci. 4, 1-21 (1966)

UNCLASSIFIED

Security Classification

DOCUMENT CONTROL DATA - R&D

(Security classification of title, body of abstract and indexing annotation must be entered when the overall report is classified)

1 ORIGINATING ACTIVITY (Corporate author) Aerospace Corporation El Segundo, California		2a REPORT SECURITY CLASSIFICATION Unclassified 2b GROUP
3 REPORT TITLE A STUDY OF BUCKLING AND SNAPPING UNDER DYNAMIC LOAD		
4 DESCRIPTIVE NOTES (Type of report and inclusive date)		
5 AUTHOR(S) (Last name, first name, initial) Lock, M.H.		
6 REPORT DATE December 1967	7a TOTAL NO OF PAGES 50	7b NO OF REFS 46
8a CONTRACT OR GRANT NO F04695-67-C-0158 b PROJECT NO c d	9a ORIGINATOR'S REPORT NUMBER(S) TR-0158(3240-30)-3 9b OTHER REPORT NO(S) (Any other numbers that may be assigned this report) SAMSO-TR-68-100	
10 AVAILABILITY/LIMITATION NOTICES This document has been approved for public release and sale; its distribution is unlimited.		
11 SUPPLEMENTARY NOTES	12 SPONSORING MILITARY ACTIVITY Space and Missile Systems Organization Air Force Systems Command Los Angeles, California	
13 ABSTRACT The behavior of a shallow arch and a thin ring under a dynamic pulse loading is studied for a wide range of geometric and load parameters. The nonlinear dynamic response and static load deflection characteristics of the systems are related and employed to define dynamic elastic snapping and dynamic elastic buckling. When such a relationship cannot be established, the mechanism of dynamic elastic-plastic buckling is introduced. Critical dynamic load criteria are specified, and critical dynamic load data are developed as a function of structural geometry and load duration. Finally, a classification scheme for dynamic load problems is suggested.		

UNCLASSIFIED

Security Classification

14

KEY WORDS

Dynamic Buckling
Critical Dynamic Loads
Pulse Loads
Elastic Stability
Dynamic Response
Dynamic Snapping

Abstract (Continued)

UNCLASSIFIED

Security Classification